Caspian J. Environ. Sci. Vol. 16 No. 4 pp. 333~347

CJES
Caspian Journal of Environmental Sciences

[Research]

Effects of wind velocity and soil characteristics on dust storm generation in Hawr-al-Azim Wetland, Southwest Iran

Adib A.*, Oulapour M., Chatroze A.

Department of Civil Engineering, Faculty of Engineering, Shahid Chamran University of Ahvaz, Ahvaz, Iran

** Corresponding author's E-mail:arashadib@yahoo.com* (Received: April 11. 2018 Accepted: Sep. 17. 2018)

ABSTRACT

Nowadays, dust storms are an important environmental problem in Iran (especially in Khuzestan Province). The Hawr-al-Azim Wetland is a source for generation of dust storms. One-third area of this wetland is located in Iran. In this study, dust discharge is calculated using wind velocity, mean soil grain size (D_{50}) and soil dry density. Soil characteristics were determined by data collected from 16 boreholes drilled in this wetland. Distributions of D_{50} and soil dry density in the wetland were determined using ordinary kriging method. Then critical wind speed was calculated in different regions of the wetland. The wetland soil is composed of medium and coarse silty soil. The dust mass discharge has reduced from 2003. The maximum monthly dust discharge mass occurs in June and July (along with a mean monthly wind velocity of 4.42 m s^{-1} and 4.27 m s^{-1}, respectively). Because of the little amount of clay particles and the high wind velocity, increased soil moisture content cannot help in neither raise inthe critical shear velocity nor decreased dust mass discharge. Also, the produced dust is transported towards Northwest Iran because the dominant direction of wind is 270° to 300° relative to the north.

Key words: Critical shear velocity, Dust mass discharge, Soil moisture content, Hawr-al-Azim Wetland, Wind erosion.

INTRODUCTION

Dust storm is a hazardous phenomenon aggravated by climatic change and global warming in recent years. In Middle East countries, such as Iran, dust storms have induced harmful influences on human societies and caused economic, social, environmental, political and security problems. Construction of large dams, extraction of petroleum, drying wetlands, destruction of straw lands, lack of specific program for protection of water and soil resources, wars and terrorist groups, have decreased the flow discharge of rivers and wetlands in Iran and Iraq. Drying wetland has decreased the vegetation cover of the region. These factors have increased the severity of dust storms in recent years (especially from 2006 thus far). The dust storms cause cardiovascular and pulmonary diseases in human, destruction of farms, reducing people's income and forcing them to migrate. The decrease in population provides favorable conditions for activities of terrorists and smugglers.

Hawr-al-Azim is a very important wetland located in the Iran and Iraq border area. Because of Iran-Iraq war, Persian Gulf wars, construction of large dams on the Tigris, Euphrates and Karkheh rivers in Iran and Turkey, petroleum production activities by Iranian oil ministry and activities of terrorist groups, the area of this wetland has reduced significantly. Dried parts of the Hawr-al-Azim Wetland are a source of dust generation. This research focuses on this source. Because of the importance of the subject, a number of

researchers have studied dust generation in the recently. Feng *et al*. (2002) studied the chemical, physical and mineralogical characteristics of sediments producing dust storm in different regions of China (e.g. the Kashi, Taklimakan desert, Kunlun Mountains, Donghuang, Lanzhou, Ningxia, Xi'an, Inner Mongolia and Beijing) during 1990 to 1994. These sediments were silty clay and clay loam and their soil D_{50}were from 5 to 63 μm. Chemical analysis showed that these sediments are SiO_2, Al_2O_3 and K_2O. Alfaro *et al.* (2004) studied the fine dust generation in arid and semi-arid regions of Niger and Southwest USA and prepared a physically explicit Dust Production Model (DPM). They reported that soil roughness length and the dry size distribution are effective parameters and soil texture is not an effective parameter on soil erosion against wind. Goudie (2008) stated that movement of fine soils by surface flows, vertical profile, wetting and drying of soil, salt heave, bioturbation, frost action, and dust accretion are effective factors on wind erosion in deserts. Goudie (2009) also studied sources of dust storms in western China and the Sahara (especially Bodélé) of Chad. He identified critical regions that are location of dust storm generation in these deserts during millennial, century, decadal, annual and seasonal periods. Goudie (2014) showed that source of dust storms are in the Sahara of Africa, central and eastern Asia, the Middle East, and parts of the western USA. These dust storms resulted in human health problems in large cities such as Phoenix, Kano, Athens, Madrid, Dubai, Jeddah, Tehran, Jaipur, Beijing, Shanghai, Seoul, Taipei, Tokyo, Sydney, Brisbane and Melbourne. Indoitu *et al.* (2012) identified sources of dust storm generation in Central Asia to be sandy desert in the large dust belt. Human activities produced harmful influences on environment of these regions and this belt included the southern deserts, north of the Caspian Sea deserts, south of Balkhash Lake, and Aral Sea region. They reported that dust storm frequency has reduced in last decades. Shao *et al.* (2013) evaluated effects of global warming on dust storm frequency and dust concentration during 1974-2012 in North Africa, the Middle East, Southwest Asia, Northeast Asia, South America, and Australia. They used different climatic indices and showed that dust concentration decreased from 1984 to 2012 because dust activity reduced in North Africa, South America, South Africa and Northeast Asia. Bryant (2013) evaluated recent developments on different aspects of dust storm studies and applied methods for identification of sources of dust storms, determination of heterogeneity in dust emissions, relation between dust storms and geomorphologic contexts and etc. Rezazadeh *et al*. (2013) showed that dust storms occur in four regions of Middle East (Sudan, parts of Saudi Arabia and Iraq, Pakistan, and also parts of Iran and Afghanistan). The maximum numbers of blowing dust and dust storm are observed over Iran and Afghanistan while the highest values of mean dust concentration are found in Pakistan. Fan *et al*. (2013) studied increased particle matter (PM_{10}) concentration during a dust storm (23-25 April 2009) in provinces of North China. They showed that source of this storm was in Mongolia and concentration of PM_{10} during dust storm was twice higher than those of non-dust storm period. Alizadeh-Choobari *et al.* (2014) studied relation between 120-daywindsand fine dust storms in Sistan Province, southeast of Iran. They illustrated that the sources of dust are in Iran and along its borders. Hamidi *et al.* (2014) simulated the severe dust event of 3–8 July 2009 in the Middle East by the WRF–DuMo model. They showed that in the Aral–Caspian Sea area, central Iran and the Dead Sea Basin, dust emission is suppressed due to the high soil-salt content. Hamidi *et al*. (2017) also studied occurred dust storm during 3-8 July 2009 in the Middle East and reported that the source of 60% of dust particles were in west of Iraq, east of Syria and northwest of Jordan while the source of 10% of dust particles were in Iran. 21% of deposited dust was deposited in Iran and 79% in other countries. Cao *et al.* (2015) evaluated social, economic and environmental impacts of dust

storms in Iran. They applied nine datasets such as temperature, precipitation and etc., combining them and identifying two main sources for dust generation in Iran (the Al-Howizeh/Al-Azim marshes and Sistan Basin). Shahraiyni *et al.* (2015) used Moderate Resolution Imaging Spectroradiometer (MODIS) images and remote sensing technique for monitoring dust storms in 2008-2009. They reported that D-parameter method is the best one for preparation of aerosol concentration maps in the Middle East. Feng *et al.* (2017) employed the Normalized Difference Vegetation Index (NDVI) and copula method for determining return period of actual spring dust storm and evaluation of effects of vegetation on generation of dust storm during 1982 to 2007 in Inner Mongolia Province, China. They showed that this return period is longer than 2 years. Wang *et al.* (2017) applied two indices for determination of number and duration of dust storms during 1978 to 2007 in Northern China. These indices included Dust Storm Frequency (DSF) and Dust Storm Event (DSE), so they considered wind speed and wind direction in DSE. Therefore results of DSE are more accurate than those of DSF. Because of global warming, extreme precipitation will increase, while wind speed will decrease at future, so that, DSF and DSE values will be reduced. Lyu *et al.* (2017) studied dust falls of three dust storms in 2010. They showed that these dust storms moved from northwestern to eastern regions of China. The ranges of dust deposition flux and soil D_{50} were 1.5-25.1 g m^{-2} and 9-26.1 μm respectively. Yue *et al.* (2017) employed MODIS imagery and an improved Brightness temperature Adjusted Dust Index (BADI) for detection of dust storm during 2000 to 2011 in the Northeast Asia. They showed that accuracy of BADI is higher than 90% for detection of dust storms. Tan *et al.* (2017) investigated occurred dust storm in East Asia from 19 through 22 March 2010. Their tools included model simulations, backward trajectories, and measurements from the Cloud-Aerosol Lidar as well as Infrared Pathfinder Satellite Observation (CALIPSO) satellite. The sources of dust storm were Western China and the Gobi desert. Deposited dust flux at these sources was 2.7 to 9 times higher than the Yellow Sea and the East China Sea. Beegum *et al*. (2018) combined a regionally adapted chemistry transport model CHIMERE and the Weather Research and Forecast (WRF) model for determination of PM_{10} concentration and aerosol optical depths (AOD) in 10 occurred dust storm from 2014 to 2017 in the Arabian Peninsula of Asia. Results of these methods were good fitness to observed data. Lee *et al.* (2009) employed MODIS imagery for identification of sources of dust storm in December 15, 2003. This storm dust occurred in the Chihuahuan Desert of Texas and New Mexico (USA) and Chihuahua (Mexico). They identified 146 point sources for dust storm generation. The most of these point sources were in pasturelands and farms. This showed importance of land use and land cover types in production of dust storms.

In this research, the following procedure is used for determination of the volume of dust discharge:

1- Collecting data on velocity and direction of wind along with soil characteristics in the area of Hawr-al-Azim Wetland.

2- Determining distribution of D_{50} of soil and soil dry density in Hawr-al-Azim Wetland by the ordinary kriging method.

3- Calculating critical shear velocity for soil erosion, shear stress developed by wind and mass of dust discharge in different months of the studied years.

4- Determining movement direction of dust storms based on dominant direction of wind.

5- Evaluating effects of soil moisture content on dust discharge mass.

MATERIALS AND METHODS

The Hawr-al-Azim Wetland

In this study, the Hawr-al-Azim Wetland is considered as the case study. It is located in Iran and Iraq between N 30° 58´- N31° 50´ and E 47° 20´- 47° 55´. The area of the part of this wetland in Iran was 64,100 ha in 1970s, while nowadays, its area is only 29,000 ha. Its total area (in Iran

and Iraq) was also 307,000 ha in 1970s, while now 102,000 ha. It is located in the North Azadegan Plain, 80 km southwest of Ahvaz City. It was fed by two tributaries of the Tigris and by the Karkheh River. The Karkheh River originates in the central zone of Zagros Mountains in West Iran. The northern and central parts of the wetland were permanent, while in the south it was largely seasonal. Variation in the land cover of Hawr-al-Azim from 1973 to 2000 is illustrated in Fig. 1 (UNEP, 2001). The nearest climatic station to its Iranian partis the Bostan station (31°43'18''N, 47°59'12''E). Mean annual temperature, precipitation and wind velocity in this climatic station are 25°C, 196 mm and 3.4 m s^{-1}, respectively. The elevation of this wetland is 5-8 meters above sea level (ma.s.l.). The general slope of this wetland is less than 0.1% from east toward west.

Methodology

In this study, the following formulas are used for calculation of dust discharge mass:

1- Calculation of critical shear velocity:

$$u_{*t} = A_t \sqrt{\frac{(\rho_s - \rho_a) g D}{\rho_a}} \quad , A_t=0.118 \qquad (1)$$

where: ρ_a is the air mass density of (1.22×10^{-3} g cm^{-3}), ρ_s is the sediment dry density, D is median size of the soil particles (cm), u_{*t} is critical shear velocity (cm s^{-1}), g is gravity acceleration (980 cm s^{-2}) (Bagnold 1941).

2- Calculation of shear velocity:

$$u_* = \alpha U_{2m} \qquad (2)$$

where: U_{2m} is the average wind speed at 2-m height above the ground (cm s^{-1}), α a coefficient equal to 0.037 for medium and coarse silt. u_* is shear velocity developed by wind (cm s^{-1}). If $u_* > u_{*t}$ then erosion will occur (Hsu 1977).

3- Calculation of dust mass discharge per unit length:

$$q = K\left[\frac{u_*}{\sqrt{gD}}\right]^3 \qquad (3)$$

where: q is dust discharge mass per unit length (gr cms^{-1}) and is K ($grcm^{-1}s^{-1}$)=$e^{-9.63+4.91D(mm)}$ according to Hsu (1977).

4- Modification of critical shear velocity based on soil moisture content:

$$\frac{u_{*tw}}{u_{*td}} = 1 \qquad for \qquad w < w'$$

$$\frac{u_{*tw}}{u_{*td}} = \left[1 + 1.21(w - w')^{0.68}\right]^{0.5} \qquad for \qquad w > w'$$

$$w' = 0.0014(\%clay)^2 + 0.17\%clay) \qquad (4)$$

where: u_{*tw} and u_{*td} are wet and dry critical shear velocity and w is soil moisture content (%)(Fécan*et al.* 1999).

Performance evaluation criteria

Root-Mean-Square Error (RMSE), Standard Error of the Mean (SEM) and Standardized Root-Mean-Square Error (SRMSE) were used for evaluation of the estimated values by ordinary kriging. The formulas of these criteria are:

$$RMSE = \sqrt{\frac{1}{n}\sum_{i=1}^{n}(Z_{i,act} - Z_{i,est})^2} \qquad (5)$$

Where $Z_{i,act}$ and $Z_{i,est}$ are actual values and estimated values by ordinary kriging respectively and n is the number of observation in 16 boreholes.

$$SEM = \frac{S}{\sqrt{n}} \qquad (6)$$

where S is the standard deviation of observed data.

$SRMSE=RMSE/S (7)

Generally, smaller RMSE and SEM values (near to zero) and a larger SRMSE value (near to one) indicate that the estimated values by ordinary kriging are better.

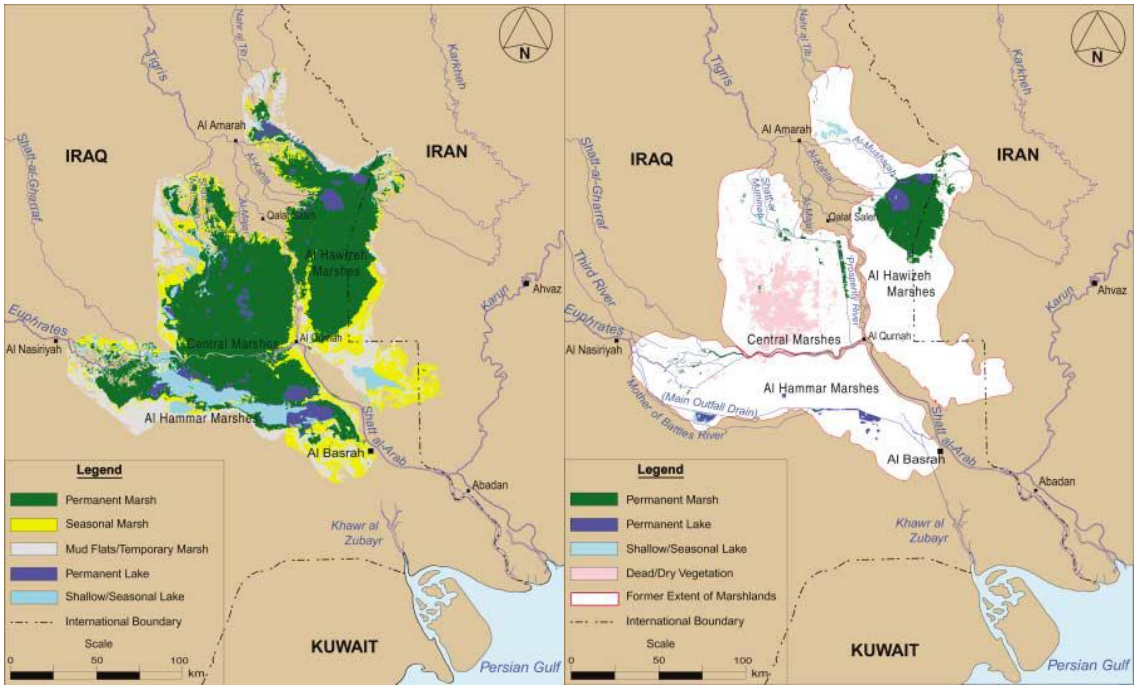

(a) (b)

Fig. 1. Variation in the land cover of the Hawr-al-Azim Wetland from 1973 to 2000 (a) 1973 (b) 2000 (UNEP, 2001).

RESULTS AND DISCUSSION

Collecting data and preparing data zoning maps by ordinary kriging method

Wind velocity

Wind velocity data were provided from Bostan Climatic Station, Khoozestan Province, Iran. The monthly mean and maximum wind velocities are illustrated in Table 1. The annual mean wind velocity was measured to be 3.41 m s^{-1}.

Wind direction

By evaluating wind direction data in the Bostan Climatic Station, it was observed that dominant direction of wind is 270° to 300° relative to the north. A sample of wind direction diagram from 2004 to 2006 is illustrated in Fig. 2.

The time interval of recording of wind velocity and direction was three hours. Fig. 2 shows percentage of different wind directions (with interval 10°). For preparation of this Fig. we considered wind velocities capable of eroding topsoil layer.

D_{50} of soil and soil dry density

In this study, collecting data on soil characteristics is conducted by drilling 16 boreholes in Hawr-al-Azim Wetland. Depth of these boreholes was almost 1 m. Soil grain gradation curves were prepared on the surface of the earth and at depths of 30, 60 and 90 cm in each borehole. The soil located on the surface of the earth (topsoil layer) was the source of dust storms, so that, soil grain gradation curves of topsoil layer were considered in this study. A sample of these curves is shown in Fig. 3. Using these gradation curves, soil D_{50} was calculated for each borehole. At the end, using ordinary kriging method, zoning map of soil $D_{50}$was determined (Fig. 4). Parameters and values of performance evaluation criteria of ordinary kriging is illustrated in Table 2. Fig. 5 exhibits the effects of partial sill, range and nugget changes on the value of RMSE of calculated soil D_{50} by ordinary kriging. This Fig. shows that the values of these parameters in Table 2 are optimum. These values minimize RMSE of calculated soil $D_{50}$by ordinary kriging. Also, using ordinary kriging method, zoning map of soil dry density was determined (Fig. 6). Parameters and values of the criteria for performance evaluation of ordinary kriging are illustrated in Table 3. Fig. 7 illustrates the

effects of partial sill, range and nugget changes on the value of RMSE of calculated soil dry density by ordinary kriging. This Fig. shows that the values of these parameters in Table 3 are optimum. These values minimize RMSE of calculated soil dry density by ordinary kriging.

Critical shear velocity

After preparing soil D_{50} and zoning maps of soil dry density, zoning map of critical shear velocity is prepared using Eq. 1. Fig. 8 shows this zoning map. This Fig. exhibits importance of soil D_{50}in determining critical shear velocity. Figs. 4 & 8 are matched and illustrate that critical shear velocity elevates as soil $D_{50}$is increased. Because of low range of variation of soil dry density, fitness between Figs. 6 & 8 is low.

Calculating dust discharge mass

Using Eq. 2, shear velocity was calculated for all data of wind velocity from 1995 to 2016. Iranian Meteorological Organization has recorded wind velocity at three hours' time steps. Then, calculated shear velocity was compared to critical shear velocity. Dust discharge mass was calculated by Eq. 3 in times and at locations that calculated shear velocity is higher than critical shear velocity. Fig. 9 shows annual dust mass discharge from 1995 to 2016. This Fig. shows an increasing trend in discharge mass from 1998 through 2003, while a decreasing one from 2003 till now (especially from 2003 to 2010). Fig. 10 illustrates that average monthly dust discharge mass occurred from 1995 through 2016 and also that the maximum value of dust discharge mass took place in June and July. In these months, wind velocity was maximum, too.

Evaluating the effects of soil moisture content on dust discharge mass

Using Eq. 4, critical shear stresses for different soil moisture contents (20%, 50% and 80%) were calculated. After modification of critical shear stress, dust discharge mass was determined using Eq. 3 for different soil moisture contents (Table 4).

Table 1. Monthly mean and maximum of wind velocity data.

Month	Jan	Feb	Mar	Apr	May	Jun	Jul	Aug	Sep	Oct	Nov	Dec
Monthly mean of wind velocity (m s^{-1})	2.81	3.12	3.45	3.6	3.72	4.42	4.27	3.85	3.18	2.8	2.89	2.83
Maximum of observed monthly wind velocity (m s^{-1})	20	50	25	22	25	26	20	16	35	24	25	16
Mean of max observed monthly wind velocity (m s^{-1})	11.89	14.39	13.96	14.5	14.62	14.69	14.31	13.14	13.9	12.41	12.59	11.59

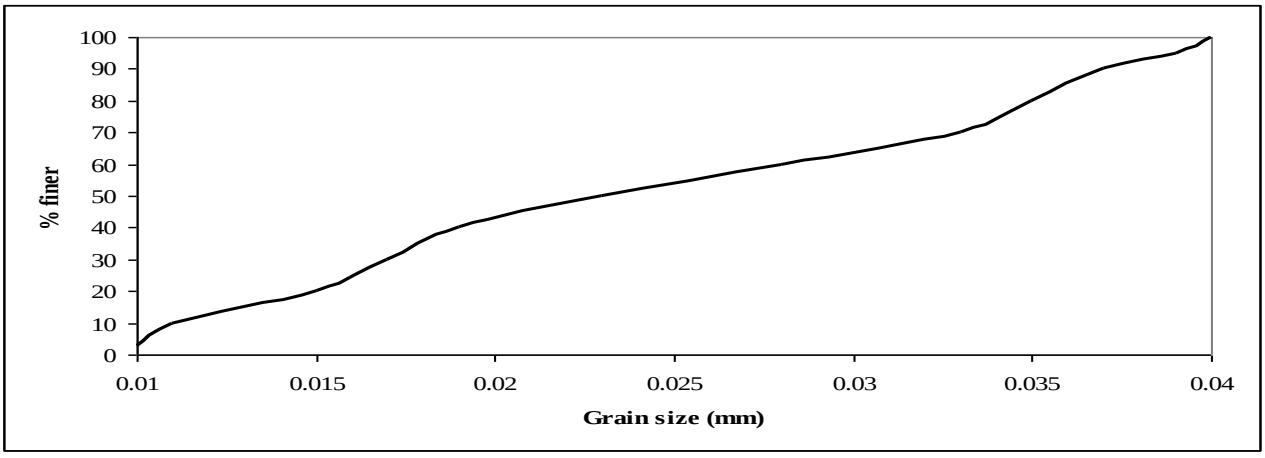

Fig. 3. A sample of soil grain gradation curves in topsoil layer.

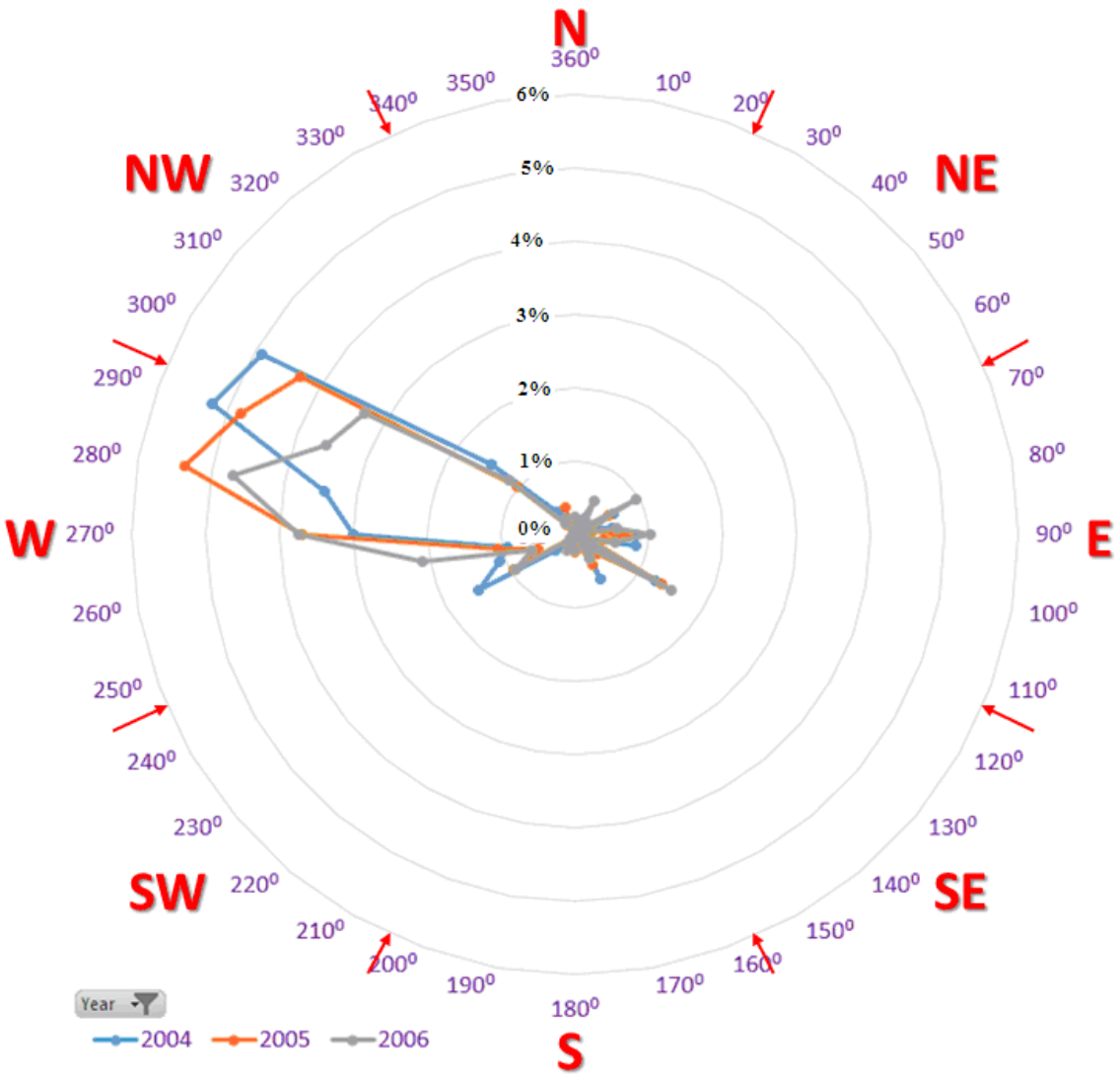

Fig. 2. Wind direction diagram from 2004 to 2006.

Table 2. RMSE, SEM, SRMSE and parameters of ordinary kriging (soil D_{50}).

Records	**16**
Searching neighborhood	Smooth
Smoothing factor	1
Major semi axis	22860.6736
Minor semi axis	22860.6736
Angle	0
Variogram	Semi variogram
Number of lags	12
Lag size	2857.5842
Nugget	1.60E-05
Model type	Gaussian
Range	22860.6736
Anisotropy	No
Partial sill	7.24E-05
RMSE (mm)	0.005499478
SEM (mm)	0.006220826
SRMSE	0.939450724

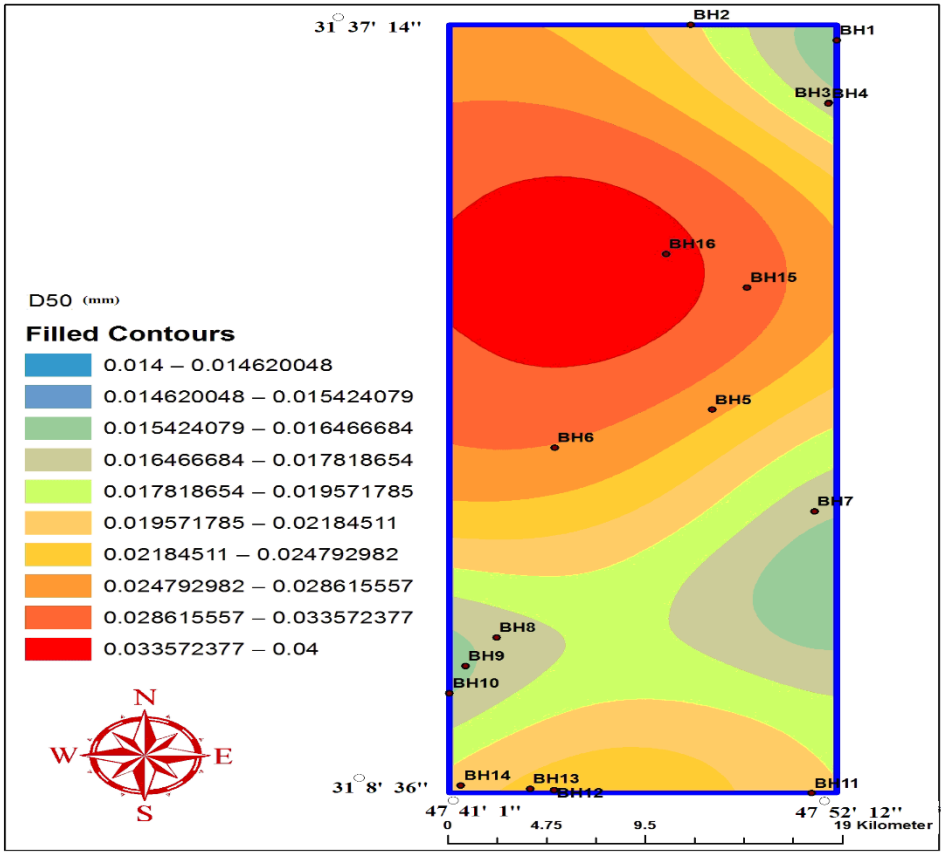

Fig. 4. D_{50} of soil zoning map.

Table 3. RMSE, SEM, SRMSE and parameters of ordinary kriging (soil dry density).

Records	**16**
Searching neighborhood	Smooth
Smoothing factor	1
Major semi axis	36383.6417
Minor semi axis	36383.6417
Angle	0
Variogram	Semi variogram
Number of lags	12
Lag size	4547.9552
Nugget	0.003537295
Model type	Gaussian
Range	36383.6417
Anisotropy	No
Partial sill	0.010435649
RMSE (gr/cm^3)	0.085083637
SEM (gr/cm^3)	0.074837787
SRMSE	0.99126107

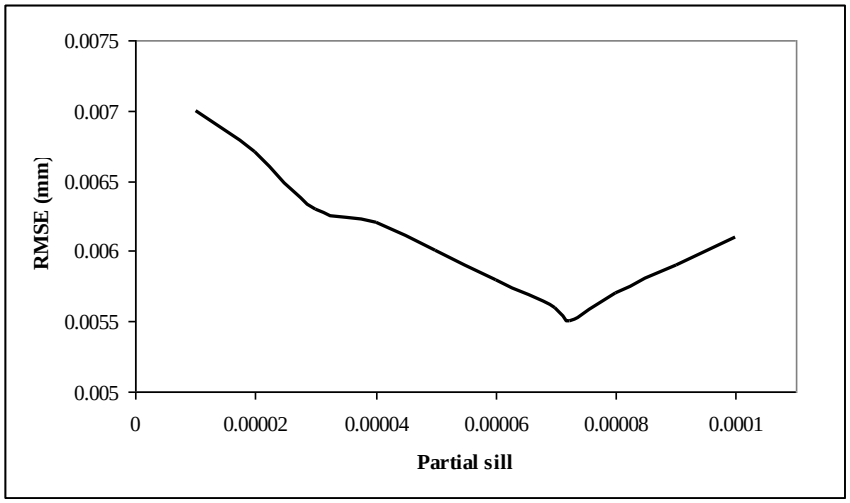

(a)

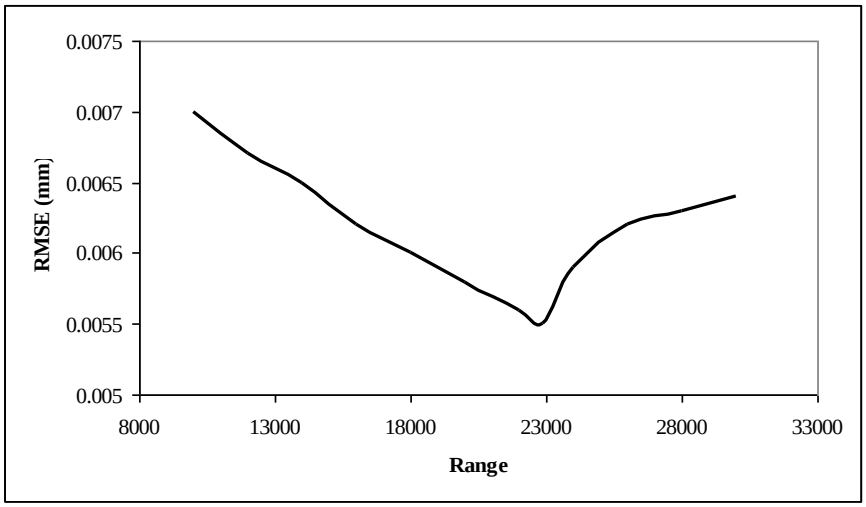

(b)

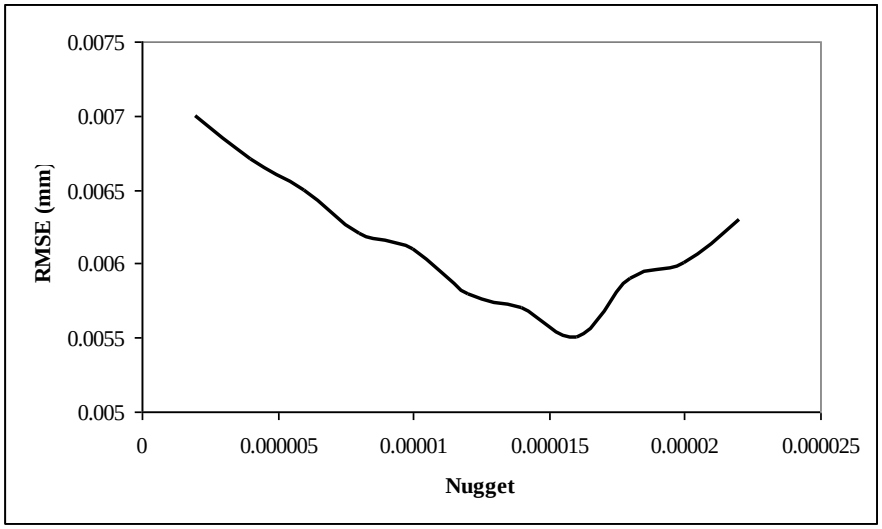

(c)

Fig. 5. The effects of changes of different parameters on the value of RMSE of calculated D_{50} of soil by ordinary kriging a) partial sill b) range c) nugget.

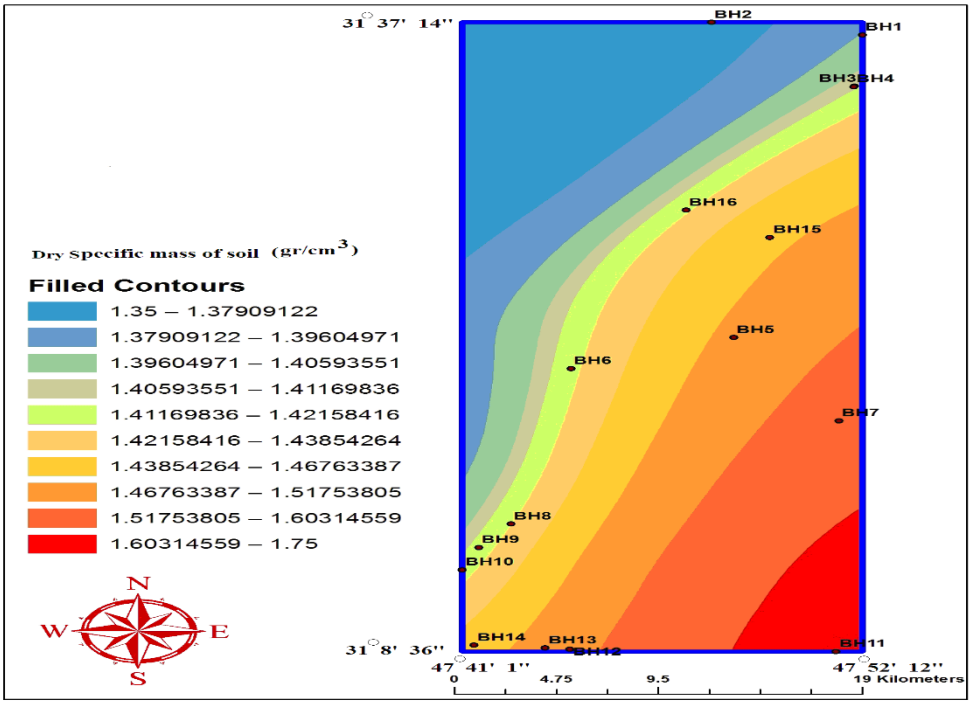

Fig. 6. Soil dry density zoning map.

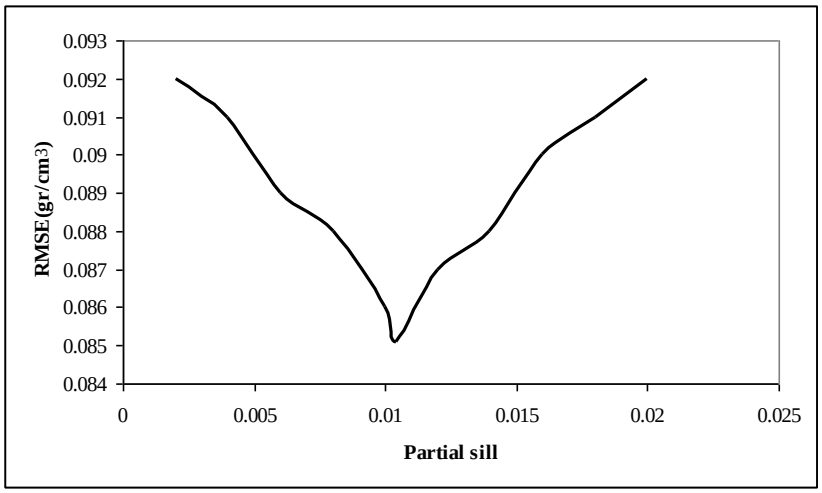

(a)

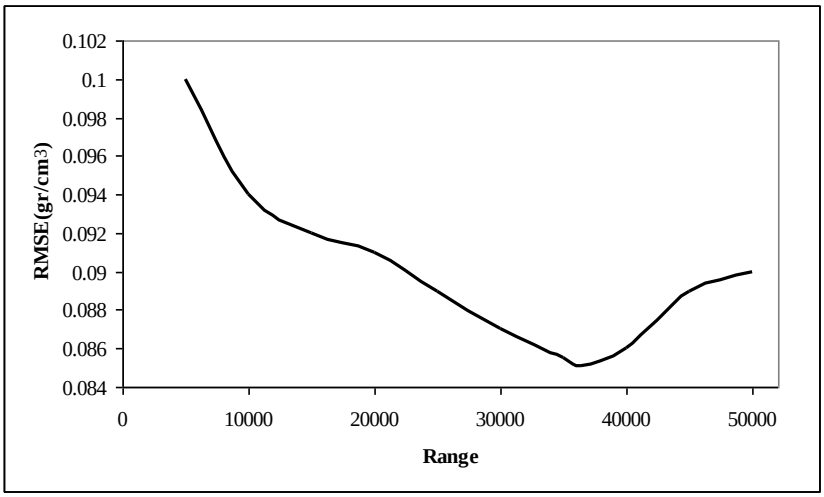

(b)

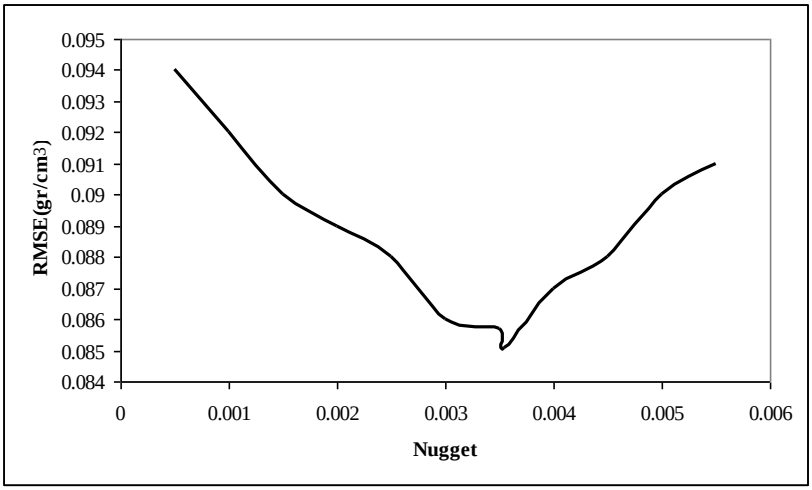

(c)

Fig. 7. The effects of changes of different parameters on the value of RMSE of calculated soil dry density by ordinary kriging a) partial sill b) range c) nugget.

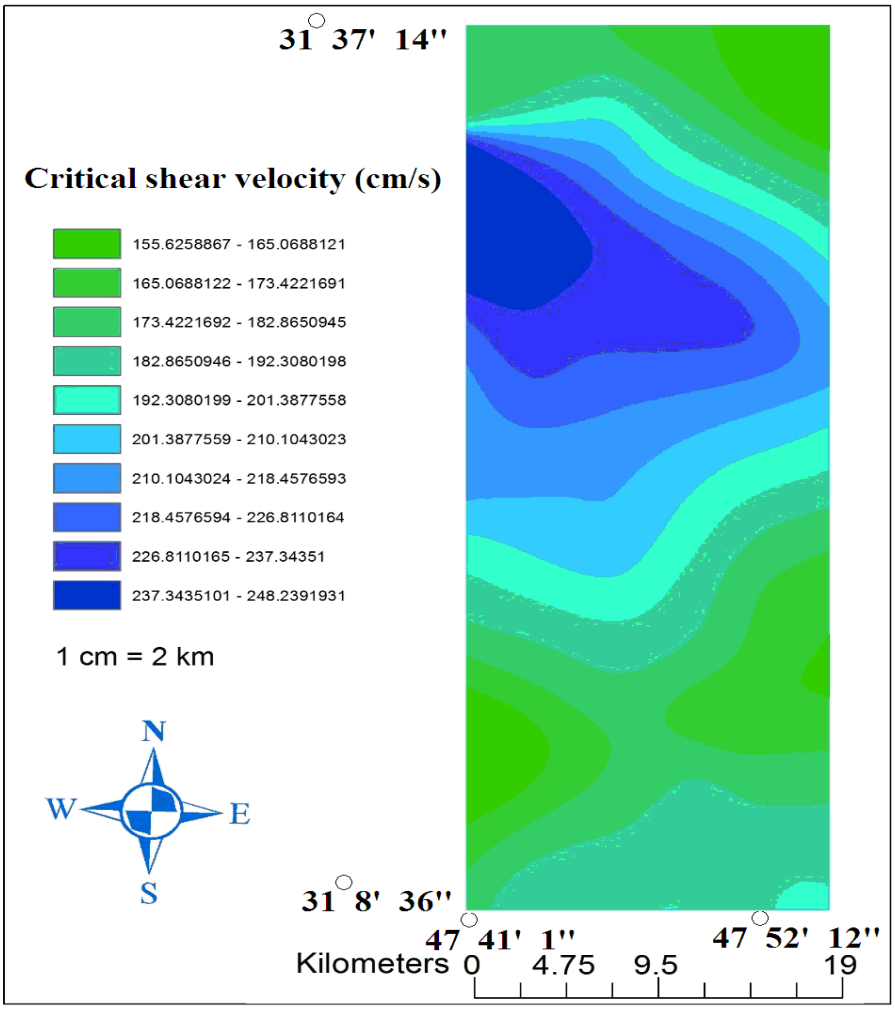

Fig. 8. Critical shear velocity zoning map.

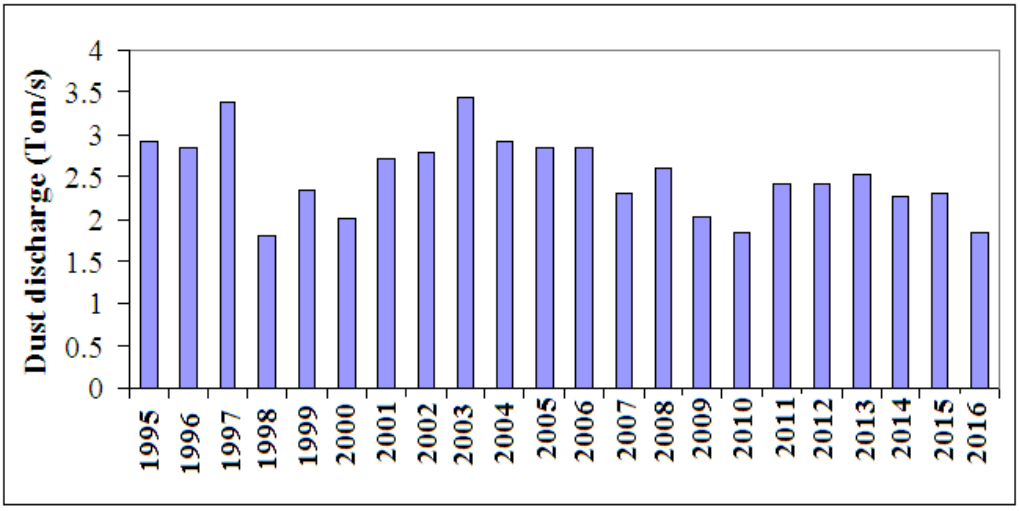

Fig. 9. Annual dust mass discharge from 1995 to 2016.

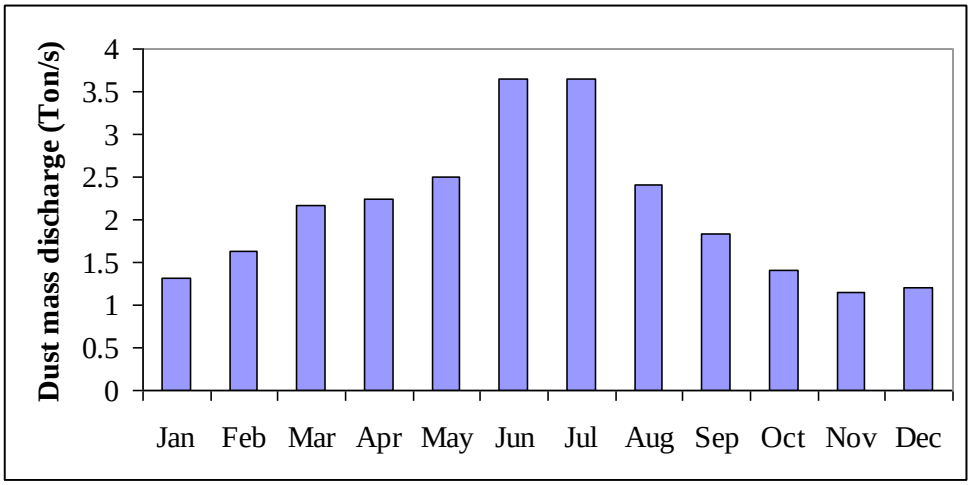

Fig. 10. Average of monthly dust mass discharge from 1995 to 2016.

Table 4. Average annual dust mass discharge from 1995 through 2016 for different soil moisture contents.

Soil moisture contents	Dry soil (0%)	20%	50%	80%
Average annual of dust mass discharge (ton s^{-1})	2.517	2.509	2.496	2.484
Ratio of change to dry soil (%)	*	-0.331	-0.851	-1.312

DISCUSSION

Table 4 exhibits that increased soil moisture content cannot reduce the soil discharge mass considerably which may be due to high values of wind velocity. The average wind velocity was higher than 3 m s^{-1} at most of the months while higher than 3.5 m s^{-1} at months that generated value of dust was very high. Notably, the most important factor in wind erosion was the average monthly maximum wind velocity. This parameter was higher than 11.5 m s^{-1} for all of the recorded months (Table 1). Fig. 8 illustrates that maximum critical shear velocity was less than 2.5 m s^{-1}. By increasing the soil moisture content up to 80%, the maximum critical shear velocity reached to 3.5 ms^{-1} only in a small part of wetland (Eq. 4). These values are much less than wind velocity and shear velocity (caused by wind). Therefore, increase in soil moisture content is not an effective factor for reducing dust discharge.

Table 1 and Fig. 10 show that the monthly dust discharge is correlated with mean monthly wind velocity. In June and July, mean and

maximum monthly wind velocity and monthly dust discharge reach their maximum values. During October to January mean and maximum monthly wind velocity and monthly dust discharge drop to their minimum values. Fig. 2 illustrates that the dust dispersion directs toward northwest (central and overcrowded regions of Iran). Therefore, adopting conservation methods against dust generation is necessary. Tables 2 & 3 display ability of ordinary kriging method for preparation of zoning maps of soil characteristics as soil dry density and D_{50} of soil.

CONCLUSION

D_{50} of soil and soil grain gradation curves of topsoil layer shows that the most of soil of the Hawr-al-Azim wetland is silt and critical shear velocity of silt is less than wind velocity in most months of year. Therefore the most important factors for calculating dust discharge mass are characteristics of wind. Other factors as soil moisture content has not much effect on dust discharge mass. The average annual dust discharge mass is almost 2.5 ton s^{-1} and this study shows that the average monthly dust discharge mass is higher than the average annual one in June and July, while it is lower than average annual one in other months which may be due to high wind speed in June and July.

This study also shows that distribution of dust storms directs toward northwest resulting in wind transfer dust toward the Khuzestan Province and other regions of Iran. The most useful approaches for confronting with dust storms seem to be reduced effects of wind on soil erosion. These approaches included planting shrubs, scattering mulch over areas which are some sources of dust particles generation and etc.

REFERENCES

Alfaro, SC, Rajot, JL & Nickling, W 2004, Estimation of PM20 emissions by wind erosion: main sources of uncertainties. *Geomorphology*, 59: 63-74.

Alizadeh-Choobari, O, Zawar-Reza, P & Sturman, A 2014, The "wind of 120 days" and dust storm activity over the Sistan Basin. *Atmospheric Research*, 143: 328-341.

Bagnold, RA 1941, The physics of blown Sand and Desert Dunes. Methuen & Co.: William Morrow, New York.

Beegum, SN, Gherboudj, I, Chaouch, N, Temimi, M & Ghedira, H 2018,Simulation and analysis of synoptic scale dust storms over the Arabian Peninsula. *Atmospheric Research*, 199: 62-81.

Bryant, RG 2013, Recent advances in our understanding of dust source emission processes. *Progress in Physical Geography: Earth and Environment*, 37: 397-421.

Cao, H, Liu, J, Wang, G, Yang, G & Luo, L 2015, Identification of sand and dust storm source areas in *Iran. Journal of Arid Land,* 7: 567-578.

Fan, Q, Shen, C, Wang, Xli, Y, Huang, W, Liang, G, Wang, S & Huang, Z 2013, Impact of a dust storm on characteristics of particle matter (PM) in Guangzhou, China. *Asia-Pacific Journal of Atmospheric Sciences*, 49: 121-131.

Fécan, F, Marticorena, B &Bergametti, G 1999, Parametrization of the increase of the aeolian erosion threshold wind friction velocity due to soil moisture for arid and semi-arid areas. *Annals of Geophysics,* 17: 149-157.

Feng, JLiN, Zhang, Z & Chen, X 2017, The dual effect of vegetation green-up date and strong wind on the return period of spring dust storms. *Science of the Total Environmen*t, 592: 729-737.

Feng, Q, Endo, KN & Cheng, GD 2002, Dust storms in China: a case study of dust storm variation and dust characteristics. *Bulletin of Engineering Geology and the Environment,* 61: 253-261.

Goudie, AS 2008, The history and nature of wind erosion in deserts. *Annual Review of Earth and Planetary Sciences*, 36: 97–119.

Goudie, AS 2009, Dust storms: recent developments. *Journal of Environmental Management*, 90: 89-94.

Goudie, AS 2014, Desert dust and human health disorders. *Environment International,* 63: 101-113.

Hamidi, M, Kavianpour, MR & Shao, Y 2014, Numerical simulation of dust events in the Middle East. *Aeolian Research*, 13: 59-70.

Hamidi, M, Kavianpour, MR & Shao, Y 2017, A quantitative evaluation of the 3–8 July 2009 Shamal dust storm. *Aeolian Research,* 24: 133-143.

Hsu, SA 1977, Boundary layer meteorological research in the coastal zone. HJ, Walker (ed.), Geoscience and Man, School of Geoscience, Louisiana State University, Baton Rouge, LA 18, pp. 99-111.

Indoitu, R, Orlovsky, L & Orlovsky, N 2012, Dust storms in Central Asia: spatial and temporal variations. *Journal of Arid Environments,* 85: 62–70.

Lee, JA, Gill, TE, Mulligan, KR, Acosta, MD& Perez, AE 2009, Land use/land cover and point sources of the 15 December 2003 dust storm in southwestern North America. *Geomorphology*, 105: 18-27.

Lyu, Y, Qu, Z, Liu, L, Guo, L, Yang, Y, Hu, X, Xiong, Y, Zhang, G, Zhao, M, Liang, B, Dai, J, Zuo, X, Jia, Q, Zheng, H, Han, X, Zhao, S & Liu, Q 2017,Characterization of dustfall in rural and urban sites during three dust storms in northern China, 2010. *Aeolian Research,* 28: 29-37.

Rezazadeh, M, Irannejad, P & Shao, Y 2013, Climatology of the Middle East dust events. *Aeolian Research,* 10: 103-109.

Shahraiyni, HT, Karimi, K, Nokhandan, MH & Moghadas, NH 2015, Monitoring of dust storm and estimation of aerosol concentration in the Middle East using remotely sensed images. *Arabian Journal of Geosci*ences, 8: 2095-2110.

Shao, Y, Klose, M &Wyrwoll, KH 2013, Recent global dust trend and connections to climate forcing. *Journal of Geophysical Research: Atmospheres*, 118: 11107–11118.

Tan, SC, Li, J, Che, H, Chen, B & Wang, H 2017, Transport of East Asian dust storms to the marginal seas of China and the southern North Pacific in spring 2010. *Atmospheric Environment,* 148: 316-328.

UNEP 2001, The Mesopotamian Marshlands: Demise of an Ecosystem. Early Warning and Assessment. Technical Report, United Nations Environment Programme, UNEP/DEWA/TR.01-3.

Wang, R, Liu, B, Li, H, Zou, X, Wang, J, Liu, W, Cheng, H, Kang, L & Zhang, C 2017, Variation of strong dust storm events in Northern China during 1978–2007. *Atmospheric Reearch* 183: 166-172.

Yue, H, He, C, Zhao, Y, Ma, Q & Zhang, Q 2017, The brightness temperature adjusted dust index: An improved approach to detect dust storms using MODIS imagery. *International Journal of Applied Earth Observation and Geoinformation,* 57: 166-176.

اثرات سرعت باد و خصوصیات خاک بر روی تولید ریزگردها در تالاب هورالعظیم، جنوب غربی ایران

ادیب الف.*، اولی پور م.، چتر روز الف.

گروه مهندسی عمران، دانشکده مهندسی، دانشگاه شهید چمران اهواز، اهواز، ایران

(تاریخ دریافت: ۹۷/۰۱/۲۲ تاریخ پذیرش: ۹۷/۰۶/۲۶)

چکیده

امروزه وقوع ریزگردها مسئله مهمی در ایران (به‌خصوص استان خوزستان) است. یکی از منابع تولید ریزگردها، تالاب هورالعظیم است. یک سوم مساحت این تالاب در ایران است. در این مطالعه دبی ریزگردها بر اساس سرعت باد، اندازه متوسط ذرات خاک و چگالی خاک خشک تعیین می‌شود. به وسیله داده‌های تهیه شده در ۱۶ گمانه حفر شده در تالاب، خصوصیات خاک تعیین شد. با روش کرجینگ معمولی توزیع اندازه متوسط ذرات خاک و چگالی خاک خشک تعیین شد همچنین سرعت بحرانی باد در نواحی مختلف تالاب محاسبه شد. خاک تالاب از جنس لای متوسط و درشت است. دبی جرمی ریزگردها از ۲۰۰۳ کاهش یافته است. حداکثر دبی جرمی ماهانه مربوط به ماه‌های ژوئن و جولای است که سرعت باد در این ماه‌ها به ترتیب ۴/۴۲ و ۴/۲۷ متر بر ثانیه است. به دلیل مقدار کم خاک رس در این ناحیه و سرعت بالای باد، افزایش رطوبت خاک نه سرعت بحرانی باد را افزایش می‌دهد و نه دبی جرمی ریزگردها را کاهش می‌دهد. به دلیل اینکه جهت باد نسبت به شمال بین ۲۷۰ تا ۳۰۰ درجه است، جهت انتقال ریزگردها به سمت شمال غربی (داخل ایران) است.

*مؤلف مسئول